energies

MDPI

Review

A Power Hardware-in-the-Loop Based Method for FAPR Compliance Testing of the Wind Turbine Converters Control

Zameer Ahmad [1], Jose Rueda Torres [1,*], Nidarshan Veera Kumar [1], Elyas Rakhshani [1], Peter Palensky [1] and Mart van der Meijden [1,2]

[1] Department of Electrical Sustainable Energy, Delft University of Technology, Mekelweg 4, 2628 CD Delft, The Netherlands; Z.Ahmad@tudelft.nl (Z.A.); N.K.VeeraKumar@tudelft.nl (N.V.K.); elyas.rakhshani@gmail.com (E.R.); P.Palensky@tudelft.nl (P.P.); M.A.M.M.vanderMeijden@tudelft.nl (M.v.d.M.)

[2] TenneT TSO B.V., 6812AR Arnhem, The Netherlands

* Correspondence: j.l.ruedatorres@tudelft.nl

Received: 6 August 2020; Accepted: 2 October 2020; Published: 6 October 2020

Abstract: A task for new power generation technologies, interfaced to the electrical grid by power electronic converters, is to stiffen the rate of change of frequency (RoCoF) at the initial few milliseconds (ms) after any variation of active power balance. This task is defined in this article as fast active power regulation (FAPR), a generic definition of the FAPR is also proposed in this study. Converters equipped with FAPR controls should be tested in laboratory conditions before employment in the actual power system. This paper presents a power hardware-in-the-loop (PHIL) based method for FAPR compliance testing of the wind turbine converter controls. The presented PHIL setup is a generic test setup for the testing of all kinds of control strategies of the grid-connected power electronic converters. Firstly, a generic PHIL testing methodology is presented. Later on, a combined droop- anFd derivative-based FAPR control has been implemented and tested on the proposed PHIL setup for FAPR compliance criteria of the wind turbine converters. The compliance criteria for the FAPR of the wind turbine converter controls have been framed based on the literature survey. Improvement in the RoCoF and and maximum underfrequency deviation (NADIR) has been observed if the wind turbine converter controls abide by the FAPR compliance criteria.

Keywords: FAPR; power hardware-in-the-loop; inertia emulation; wind turbine; converter control

1. Introduction

A gradual decommissioning of the fossil-fuel fired generation plants and their controls is a challenge to the stable operation and control of the electric power system. Without implementation of necessary mitigation measures to tackle the reduction of system inertia and the absence of robust conventional primary frequency control attached to synchronous generations, future electric power systems may face a high RoCoF and NADIR [1].

In this context, advanced controllers for fast active power-frequency control are needed to quickly and effectively adjust the active power at the alternative current (AC) side of the power electronic converters (e.g., voltage source converters) used to interface renewable energy-based generation systems and responsive loads (e.g., electrolysers) [2,3].

FAPR enables the controlled source to modulate its output power rapidly to arrest the frequency deviation. Depending on the system requirements, the recovery time may be bounded to be within a relatively short period [4,5]. A detailed discussion on the limits and possible trade-off between the consumed energy from the FAPR controller and the recovery time can be found in

the work by Dreidy et al. [4]. FAPR controllers are mainly grouped into three categories, namely, proportional/droop-based controllers [6–9], derivative-based controllers [10–13], and other methods, which are mainly based on the swing equation of synchronous generators, thus trying to emulate inertia through Virtual Synchronous Machine (VSM) [14–18]. Frequency regulation during sudden load variations requires a series of control actions to be performed. Hence, the combined actions of FAPR controllers offer an attractive option for the PE-based wind generation units. The first implemented controller is the droop-based approach, which is known as one of the most common and easy to implement controls. The droop-based controller by itself can mainly contribute to the improvement of NADIR value, and not to mitigate changes of RoCoF. This is because the droop-based controller takes the frequency error as input, which is multiplied by a gain (tuned on a system-dependent case). Since the droop-based controller modulates the active power injection in a slow fashion, it cannot cause an impact during the inertial response stage. However, the derivative controller can impact RoCoF since the output becomes a high sloped ramp signal, which stimulates earlier and activates control action during the inertial response stage, thus improving the frequency of RoCoF. The droop and the derivative controllers can operate in parallel at different time zones once the frequency deviation is detected. The last approach implemented within the FAPR controller package is the virtual synchronous power (VSP) controller. This controller is much versatile compared to the droop and derivative controllers. The objective of the VSP controller still remains the same as that of the droop and derivative controller, which is to improve the frequency of NADIR and RoCoF. However, this controller provides a single solution, simultaneously influencing both NADIR and RoCoF. This is possible due to the 2nd order characteristics of the VSP approach, which gives access to quickly control both overshoot and damping. Moreover, VSP has a power deviation as an input, which is more dynamic compared to frequency.

The above-mentioned characteristic of power electronic converters along with the substantial developments in digital communication networks and protocols last a few years, made possible by wind converters control testing in laboratory conditions. Adopting the PHIL testing methodology entails a precise reproduction of the wind generators' actual operating responses, as a necessary step before large-scale deployment of such converters' controls in actual power systems. Traditionally, testing of converters control strategies has been conducted directly on physical equipment in the field or on a power testbed in a lab. While offering testing accuracy, this method can be very inefficient, expensive, and dangerous. A feasible option is PHIL based compliance testing which offers an excellent alternative to traditional testing methods. PHIL simulation has become the standard for many industries due to its advantages such as highly efficient, repeatability, safety, scalability, and cost effectiveness.

In this paper, FAPR control strategies are tested through a generic PHIL based test bench. The PHIL test setup has been developed at TU Delft. The test setup consists of a real-time target (RTT), grid emulator (back-to-back converter), NovaCor real-time digital simulator (RTDS), and a DC-AC converter (DUT). The detailed discussion on PHIL testing has been presented in Section 3.

The sections of the paper are organised as follows. The proposed generic definition of FAPR is presented in Section 2. In Section 3, the PHIL test setup description and generic test methodology are discussed. Section 4 presents the FAPR compliance criteria of wind turbine converter controls. Testing of the FAPR converter controls through PHIL is discussed in Section 5. Section 6 concludes the paper.

2. Proposed Generic Definition of FAPR

Fast active power regulation (FAPR) is a control action applied to power electronic converters used to interface renewable generation, storage, or responsive demand. It involves a continuous measurement of grid frequency and/or active power deviation within very small-time frames, followed by a given action of a given controller scheme to regulate the injection/absorption of instantaneous active power to mitigate the frequency deviation caused by an imbalance. FAPR considers technical limitations or boundaries determining the capability of the controller to provide a fast frequency response.

Figure 1 illustrates the time frame of different frequency control tasks. The time frame of operation of FAPR may ideally be concurrent with the typical time frame of the generator's response of

inertial (e.g., 500 ms from the disturbance of active power). According to [19], the period highlighted with dark orange corresponds to the action of inertial response, as a consequence of a variation of the electromagnetic coupling between synchronous generators of an interconnected power system, due to a perturbation of the system's active power balance. According to [20], FAPR can support the primary frequency response in Zone A, as shown in Figure 1.

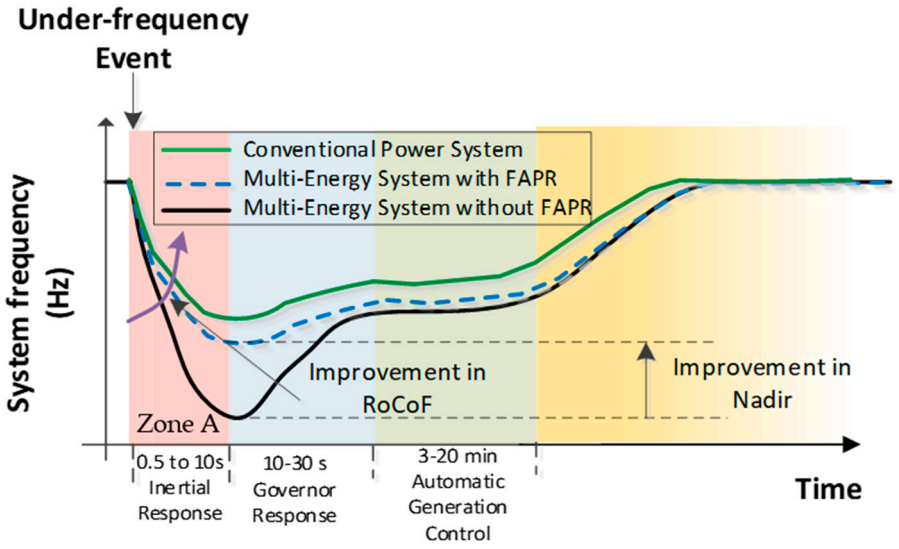

Figure 1. Expected influence of fast active power regulation (FAPR) in under-frequency events.

3. PHIL Test Setup

3.1. Description of Test Setup

The PHIL test setup for testing of power electronic converters control strategies has been developed at Delft University of Technology, IEPG, Netherlands, and RTDS lab, as shown in Figure 2. The test setup consists of real-time target (RTT), NovaCor real-time digital simulator, aurora communication protocol, device under test (DUT), and grid emulator.

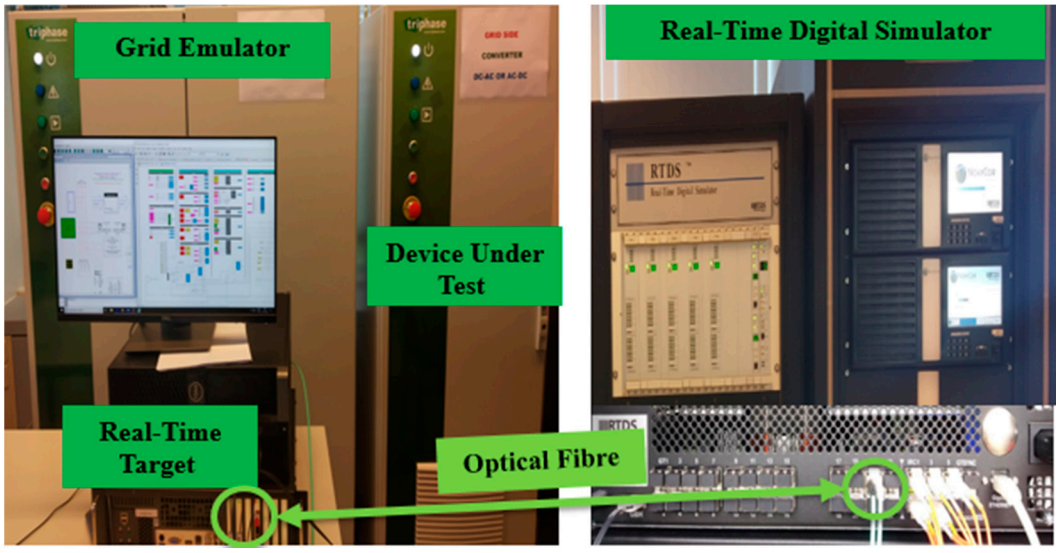

Figure 2. The power hardware-in-the-loop (PHIL) test setup.

The description of the PHIL test setup components are as follows.

3.1.1. NovaCor Real-Time Digital Simulator

NovaCor is the latest technology of the RTDS simulator, its previous version was the PB 5 card [21]. NovaCor is based on a multicore processor, which makes it the fastest real-time simulator. Various power system nodes can be evaluated on a single NovaCor. RTDS is one of the most important components of the PHIL test setup. It provides a function of connecting external physical devices to the power system running on it. By connecting the physical equipment/devices to the RTDS real-time simulation, the behaviour of the device and its impact on the simulated power system can be analysed. In this test setup, RTDS communicates with an external device through the aurora communication protocol. The aurora firmware is installed at one of the RTDS racks. RTDS and the external devices are connected through an optical fibre and exchange the information through an aurora protocol.

3.1.2. Real-Time Target

The Triphase, real-time target has an operating system based on the Linux/Xenomai. The real-time inter-PC interface assists the real-time target to connect in real-time to other real-time simulators such as the RTDS, OPAL-RT OP5600, and external control units. This enables the creation of PHIL setups, as well as the supervisory control of clusters of power module (PM) systems.

3.1.3. Grid Emulator Power Module

It is a back-to-back (B2B) converter, consisting of an active front-end converter and a voltage source converter. The front-end converter is connected to the grid. Its main function is to keep the dc link voltage constant, while the voltage source converter produces the desired voltage and frequency at its terminals.

3.1.4. Device under Test

It is a dc-ac converter. It has an active and reactive power current reference as a set-point. The active and reactive power injection into the power grid depend on the control strategy and grid operating parameters (voltage and frequency). The reference current can be set locally or from other real-time processors.

3.2. Generic Converters Control PHIL Testing Methodology

The steps adopted for the control methods testing on PHIL of the grid connected converters are as follows. For the better understanding of the terms used in the methodology, an illustrative figure is provided in Figure 3.

1. Development of the power system model on an EMT based software RSCAD [22] and the power system model is compiled to execute on the RTDS NovaCor. RTDS facilitates the connection of external devices to the simulated power system.
2. The MATLAB/Simulink environment has been used for the software model development of the DUT and grid emulator. These models are compiled and executed on a real-time target (RTT). The output of DUT and grid emulator are controlled through set-points. The set-points of DUT and grid emulator are Id, Iq, voltage, frequency, and harmonics, respectively.
3. The set-points for the DUT and grid emulator are obtained from the RTDS through an aurora protocol.
4. The RTDS and external device, as well as the RTT are physically connected by an optical fiber and exchange the information through an aurora communication protocol. The RTT uses a circular inter-process communication (CIPC) buffer. CIPC is a shared memory strategy based on ring-buffers to allow MATLAB/Simulink models to communicate with each other and other processors. A standard Simulink model using buffers as a communication infrastructure has a write functionality and/or a read functionality. To interpret the data in the buffers correctly,

the read and write blocks in Simulink make use of bus definitions. In this developed test setup, there can be an exchange of 256 signals between RTDS and RTT.

5. In order to emulate the simulated grid running in RTDS by the external device grid emulator, the voltage and frequency of the bus of the simulation network where external devices are to be connected, are sent from RTDS to RTT. RTT controls the grid emulator and generates the simulated grid behaviour at the output terminal of the grid emulator.
6. FAPR control strategies can be implemented either on MATLAB or the RSCAD software. The implemented FAPR control strategies generate a current reference for active power generation. The DUT, which is a mock-up VSC, is virtually connected to the grid (which is running on RTDS), and injects active power towards the grid emulator depending on the applied FAPR control strategy.

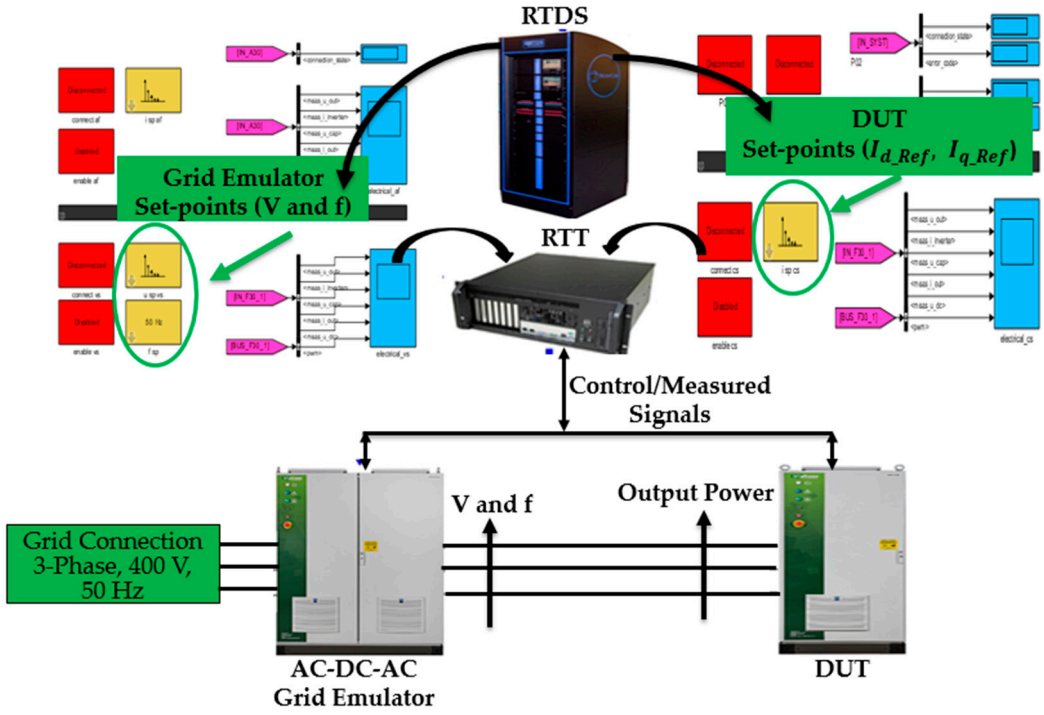

Figure 3. Working illustration of the PHIL methodology.

4. Criteria for Compliance Testing

The FAPR control methods should satisfy the following conditions, defined here based on requirements given in [23–26]. These requirements can be adjusted depending on the type and size (e.g., kW or MW wind generator) of the source of active power, and the properties of the transmission grid to which it will be connected.

1. The frequency of ROCOF and NADIR should comply with the grid code requirement (e.g., 0.5 Hz/s for ROCOF, 49.2 Hz for NADIR) for the outage of the biggest generation unit.
2. The FAPR control should respond according to the controller gain to inject the amount of power. The gain is tuned depending on the amount of the available active power.
3. At all times the control will be able to increase or decrease the active power injected into the network within a range of ΔPmax from the steady state active power output value prior to the disturbance. The value of ΔPmax depends on the technology of a specific manufacturer. According to the existing literature, as an indicative reference value, it may be considered that the value of ΔPmax can be adjusted between 0 and 10% of the maximum capacity of the grid interfacing power electronic converter.

4. If the FAPR controller is implemented separately with the storage, then, the injected active power depends on the storage capacity and power requirements to the grid.
5. After triggering FAPR, the response speed should be 500–700 ms (the rise time of injected active power, which is illustrated later with an actual simulation in Section 5). The installation can increase or decrease the active power in at least a value of 10% of the maximum capacity of the grid interfacing power electronic converter (if the grid interfacing power electronic converter is operating at its rated output and the same converter is used for power injection by FAPR).
6. Must be able to supply an energy equivalent to 5–10% of the grid interfacing power electronic converter's maximum capacity for 8–15 s, as illustrated later with an actual simulation in Section 5 [27]. After this period, it is expected that the primary frequency containment reserves operate and depending on the recovery strategy, the FAPR controller can be deactivated. The duration of FAPR can be adjusted for instance, by using a coordinated strategy [28].
7. Controllers should have a frequency insensitivity band between ±10 to ±50 mHz (depending on the stiffness of the grid) [29].
8. This control should not contribute negatively to the damping of power oscillations of the electrical system.

5. Testing of FAPR Converter Control Through PHIL

In this section, a combined droop- and derivative-based FAPR control method is tested on the PHIL setup presented in Section 3. The combined droop- and derivative-based FAPR is a control strategy, which modulates injected active power according to the derivative of deviation of the frequency from its nominal value. The combined droop- and derivative control-based FAPR implementation in the RSCAD software is depicted in Figure 4. The error in frequency is fed to the derivative controller as input, which is passed through the dead-band, here the dead-band is of negligible value because the immediate response of the controller is a priority during the containment period. Further, the frequency error signal is applied to the derivative block, which has been realized by combining a low pass Butterworth filter and first-order washout filter. The cutoff frequency of the low pass Butterworth filter is 0.5 Hz. The time constant and gain of the washout filter are 10^{-5} s and 8×10^{-5} s, respectively. The parameters of the combined droop and derivative controller is selected depending on the amount of power to be regulated.

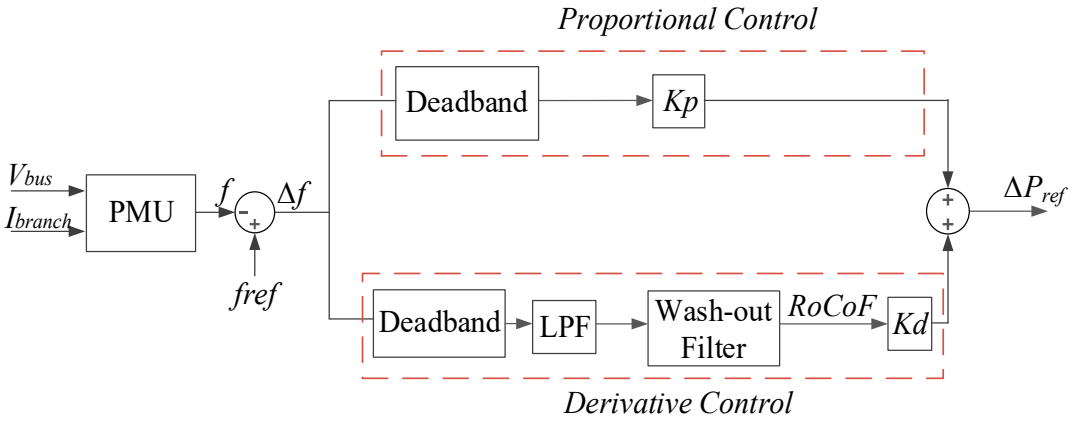

Figure 4. Combined droop- and derivative-based FAPR control.

Further, this signal is multiplied with a user-defined gain called derivative gain K_d, which shall define the response sensitivity of the derivative block. However, the derivative control block alone cannot mitigate the frequency discrepancy, because the derivative block output will only be active during a large dynamic frequency deviation and for the rest of the time (i.e., for example, when the frequency is settled at 49.6 Hz due to the load imbalance after the point of NADIR) the result of

the derivative block shall be zero. Therefore, a cascaded droop and derivative block need to be active for improvement in both NADIR and RoCoF.

The controller gains kp and kd values are selected by the sensitivity analysis. Figure 5 shows the frequency dynamics for the various values of the controller gains Kp and Kd of the combined droop- and derivative-based FAPR controller. It can be observed that at Kp = 0.73 and Kd = 0.68, the dynamic is oscillatory. For the power system under study, the value of Kp = 0.9 and Kd = 0.4 has been selected.

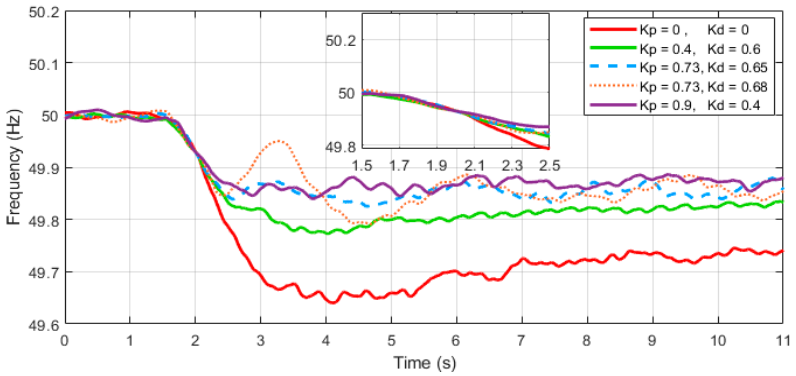

Figure 5. Selection of controllers gains kp and kd for the system under study.

The power system considered under this study is a modified IEEE (Institute of Electrical and Electronics Engineers) 9-bus system, which is used to test the controllers with the topology depicted in Figure 6. The conventional IEEE 9-bus system is altered by adding two wind power plants which contribute 52% of the power share. It is noteworthy that the wind turbine models used here are full scale not aggregate models. Table 1 describes the load flow results of the modified IEEE 9 bus system that is given in Table 1. Moreover, it is worth mentioning that the total generation and load balance has been maintained as the same as a standard IEEE bus system. The penetration of renewables has not been increased just by increasing the active power from the wind turbines but rather replacing synchronous generators. At each generation and load bus, the integrity of voltage and active power balance has been maintained similar to the standard IEEE 9 bus system.

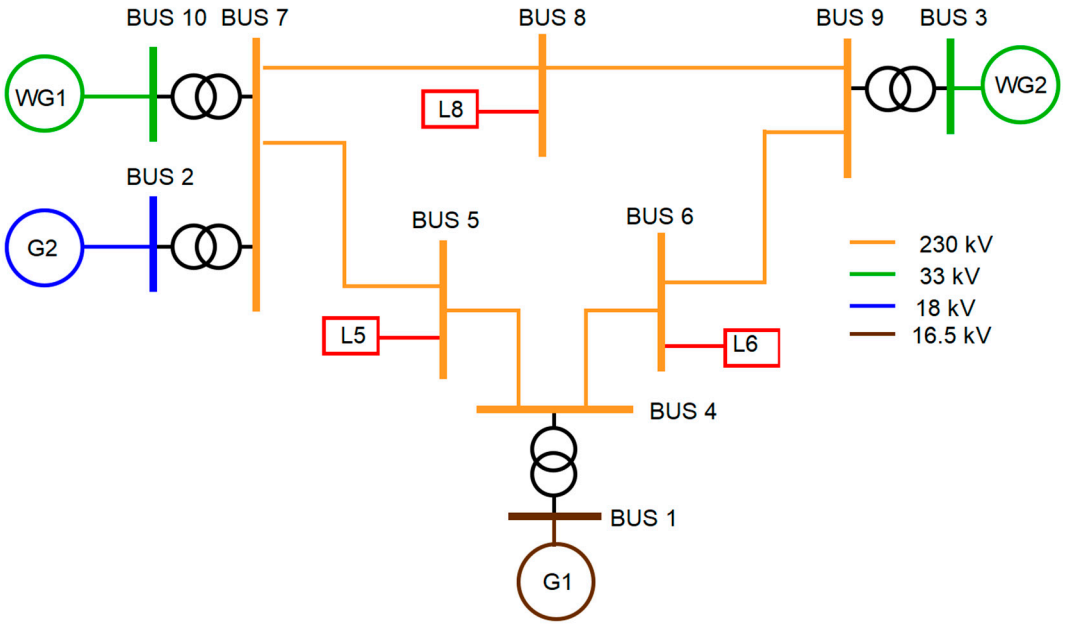

Figure 6. Modified IEEE 9 bus model with a 52% wind generator share.

Table 1. Load flow results of the modified IEEE 9 bus system.

Component	G1	G2	WG1	WG2	L5	L6	L8
MW	73.4	78.2	82.6	84	125	90	100
MVAr	33.8	−1.8	0	0	50	30	35

The combined droop- and derivative-based FAPR control strategy has been tested on the PHIL test setup under the following conditions: (a) Device under test is connected at bus 7 (Figure 6), (b) the power system is a modified IEEE 9 bus system that has a 52% penetration of type-IV wind power generation, as given in Figure 6, (c) a 5% sudden increase in the load at bus 8 (Figure 6) and (d) FAPR controller is active for 10 s. The steps adopted for the testing of FAPR through PHIL are as follows.

1. Development of the power system model (modified IEEE 9 bus system) on an EMT-based software RSCAD [22] and the power system model is compiled to execute on the RTDS NovaCor.
2. In order to emulate the behaviour of bus 7 at the output terminals of the grid emulator, the voltage and frequency of bus 7 of the modified IEEE 9 bus system at which the type 4 wind generator is connected was sent from RTDS to RTT through an aurora protocol, as depicted in Figure 7. The active power for the DUT is taken from the local grid at 400 V and 50 Hz RMS. The grid emulator is a back-to-back (B2B) converter. The output of grid emulator is connected to the AC side of the DUT, as shown in Figure 7. The DC side of the DUT is connected to the dc bus of the B2B link of grid emulator.
3. As RTDS and the real-time target both are running in real-time, the combined droop- and derivative-based FAPR control method was implemented in RSCAD. The current reference generated by the FAPR controller for the injection of active and reactive power are Id_ref and Iq_ref. These current references were fed to the device under test, as shown in Figure 7. The device under test output power depends on the value of the current reference. The signals corresponding to the three phase output current of the DUT is fed to the simulated grid, as shown in Figure 7.

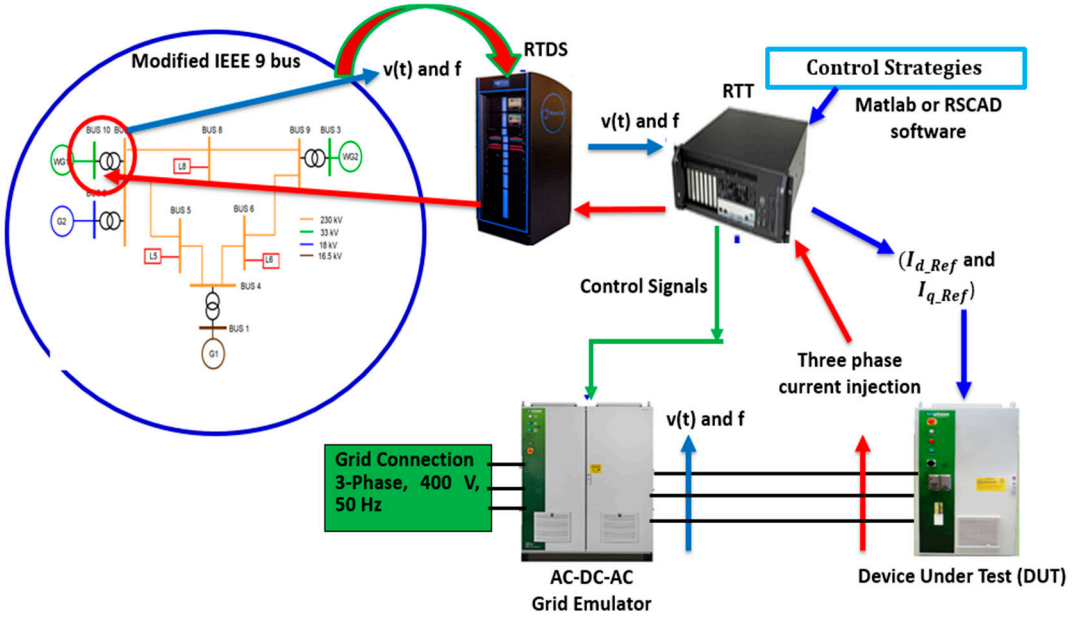

Figure 7. Illustration of FAPR control testing through PHIL.

From Figures 8 and 9, the dynamics of the active power injection by the combined droop- and derivative-based FAPR control method and its counter effect on the frequency can be seen. In addition, the active power injection and frequency curves are complying with the compliance

criteria for FAPR, as discussed in Section 4. The frequency NADIR and RoCoF are within the defined limit. NADIR is improved from 49.64 to 49.82 Hz. While ROCOF is improved from 0.28 Hz/s to 0.04 Hz/s. The gain of the controller is tuned (K = 1 pu) to inject 10% of the rated power. It is injecting 10% of the rated power. After a few seconds, the power injection decreases due to a decrease in the requirement of power and improvement in the frequency. The rise time of active power is 510 ms, which is within the specified limit. The FAPR controller is active for 10 s. The frequency insensitivity band of ±30 mHz has been considered. The power system is stable and the implemented FAPR has not contributed negatively to the damping of power oscillations of the electrical system.

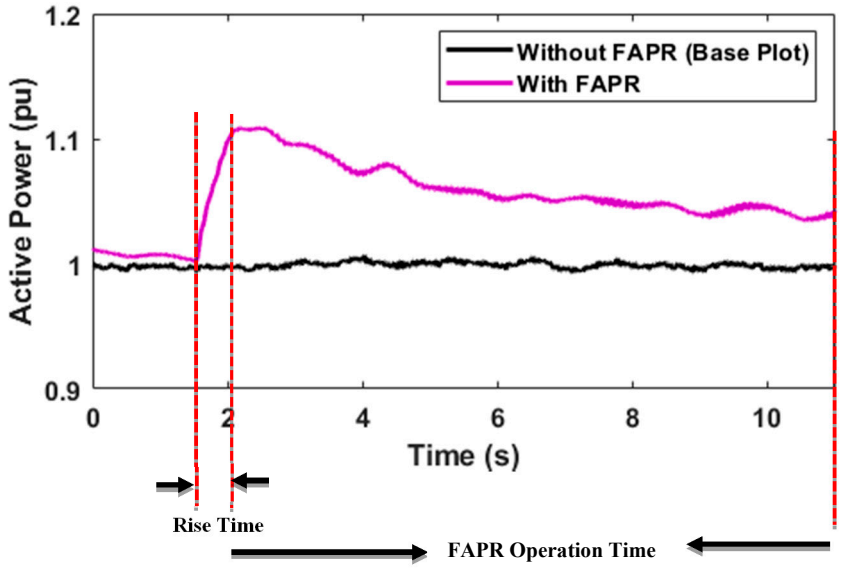

Figure 8. Illustration of FAPR control testing through PHIL.

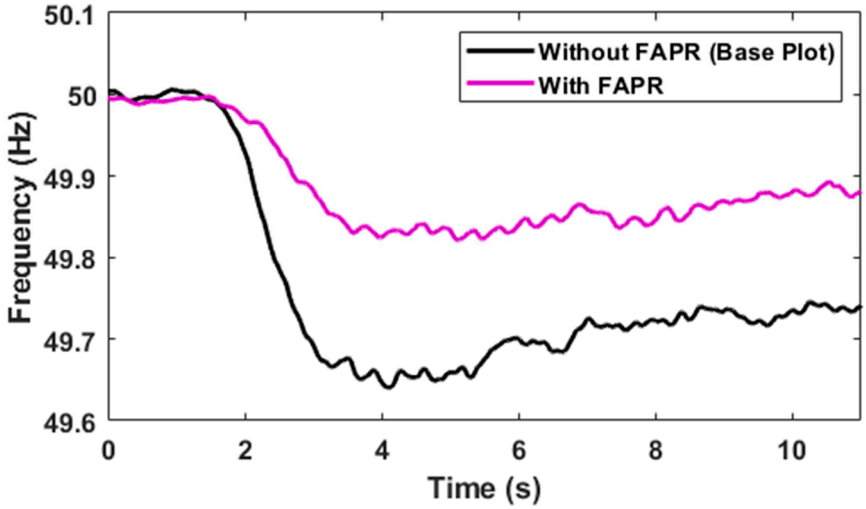

Figure 9. Dynamics of frequency due to the FAPR controller.

6. Conclusions

In this study, a power hardware-in-the loop (PHIL) based method for FAPR compliance testing of the wind turbine converter controls has been presented. The test setup consists of a real-time target (RTT), grid emulator (back-to-back converter), NovaCor real-time digital simulator (RTDS), a dc-ac converter (device under test), and an aurora communication protocol. Based on the literature survey, the compliance criteria for the FAPR of the wind turbine converters have been outlined. The developed PHIL based test method is applicable for all kinds of the grid connected converter

control. There is flexibility in the implementation of control strategies. It can be implemented in RSCAD or the MATLAB/Simulink software. It is safer, as there is no electrical connection between RTDS and the converters. They are connected through an optical fiber. Multiple converters can be tested, as it has 256 signals exchange at a time. Furthermore, it is extendable. The rise time of active power injected by the real converter (device under test) is 510 ms, which is within the specified limit of FAPR. The improvement in RoCoF and NADIR was observed due to the power injected by the FAPR control of the wind turbine.

Therefore, the presented PHIL testing method of converter controls is an efficient method for testing in laboratory conditions before employment in the actual power system. An analysis from the pure device point-of-view, involving for instance, the time varying current injection, harmonic distortion, and grid synchronization technique will be reported in the future publication.

Author Contributions: Conceptualization, Z.A., N.V.K., J.R.T. and E.R.; formal analysis, Z.A., N.V.K., J.R.T. and E.R.; investigation, Z.A., N.V.K., J.R.T. and E.R.; methodology, Z.A., N.V.K., J.R.T. and E.R.; resources, Z.A., N.V.K., J.R.T. and E.R.; software, Z.A. and N.V.K.; supervision, J.R.T., E.R., P.P. and M.v.d.M.; validation, Z.A., NV.K., J.R.T. and E.R.; visualization, Z.A. and N.V.K.; writing—original draft, Z.A., NV.K., J.R.T. and E.R.; writing—review & editing, Z.A., NV.K., J.R.T., E.R., P.P and M.v.d.M. All authors have read and agreed to the published version of the manuscript.

Funding: This research was carried out as part of the MIGRATE project. This project has received funding from the European Union's Horizon 2020 research and innovation program, under grant agreement no. 691800. This reflects only the authors' views, and the European Commission is not responsible for any use that may be made of the information it contains.

Conflicts of Interest: The authors declare no conflict of interest. The funders had no role in the design of the study; in the collection, analyses, or interpretation of data; in the writing of the manuscript, or in the decision to publish the results.

References

1. Blaabjerg, F.; Ma, K. Future on Power Electronics for Wind Turbine Systems. *IEEE J. Emerg. Sel. Top. Power Electron.* **2013**, *1*, 139–152. [CrossRef]
2. Chen, Z.; Guerrero, J.M.; Blaabjerg, F. A Review of the State of the Art of Power Electronics for Wind Turbines. *IEEE Trans. Power Electron.* **2009**, *24*, 1859–1875. [CrossRef]
3. Blaabjerg, F.; Ma, K. Power electronics converters for wind turbine systems. *IEEE Trans. Ind. Appl.* **2012**, *48*, 708–719. [CrossRef]
4. Dreidy, M.; Mokhlis, H.; Mekhilef, S. Inertia response and frequency control techniques for renewable energy sources: A review. *Renew. Sustain. Energy Rev.* **2017**, *69*, 144–155. [CrossRef]
5. Hafiz, F.; Abdennour, A. Optimal use of kinetic energy for the inertial support from variable speed wind turbines. *Renew. Energy* **2015**, *80*, 629–643. [CrossRef]
6. Mishra, S.; Zarina, P.P.; Sekhar, P.C. A novel controller for frequency regulation in a hybrid system with high PV penetration. In Proceedings of the 2013 IEEE Power & Energy Society General Meeting, Vancouver, BC, Canada, 21–25 July 2013; pp. 1–5.
7. Josephine, R.; Suja, S. Estimating PMSG Wind Turbines by Inertia and Droop Control Schemes with Intelligent Fuzzy Controller in Indian Development. *J. Electr. Eng. Technol.* **2014**, *9*, 1196–1201. [CrossRef]
8. Yao, W.; Lee, K.Y. A control configuration of wind farm for load-following and frequency support by considering the inertia issue. In Proceedings of the 2008 IEEE Power and Energy Society General Meeting-Conversion and Delivery of Electrical Energy in the 21st Century, Detroit, MI, USA, 24–28 July 2011; pp. 1–6.
9. Engelken, S.; Mendonca, A.; Fischer, M.; Engelken, S. Inertial response with improved variable recovery behaviour provided by type 4 WTs. *IET Renew. Power Gener.* **2017**, *11*, 195–201. [CrossRef]
10. Satapathy, P.; Debnathm, M.K.; Mohanty, P.K. Design of PD-PID Controller with Double Derivative Filter for Frequency Regulation. In Proceedings of the 2018 2nd IEEE International Conference on Power Electronics, Intelligent Control and Energy Systems (ICPEICES), Delhi, India, 22–24 October 2018; pp. 1142–1147. [CrossRef]

11. Gonzalez-Longatt, F.; Chikuni, E.; Stemmet, W.; Folly, K. Effects of the Synthetic Inertia from wind power on the total system inertia after a frequency disturbance. In Proceedings of the 2013 IEEE International Conference on Industrial Technology (ICIT), Johannesburg, South Africa, 9–13 July 2013; pp. 826–832.
12. Ackermann, T. *Wind Power in Power Systems*, 2nd ed.; Wiley: Hoboken, NJ, USA, 2005; Volume 140.
13. Rakhshani, E.; Rodriguez, P. Inertia Emulation in AC/DC Interconnected Power Systems Using Derivative Technique Considering Frequency Measurement Effects. *IEEE Trans. Power Syst.* **2017**, *32*, 3338–3351. [CrossRef]
14. Rakhshani, E.; Remon, D.; Cantarellas, A.M.; Garcia, J.M.; Rodriguez, P. Virtual Synchronous Power Strategy for Multiple Power Systems. *IEEE Trans. Power Syst.* **2017**, *32*, 1665–1677. [CrossRef]
15. Zhong, Q.-C.; Weiss, G. Synchronverters: Inverters That Mimic Synchronous Generators. *IEEE Trans. Ind. Electron.* **2010**, *58*, 1259–1267. [CrossRef]
16. Beck, H.-P.; Hesse, R.; Beck, I.H.-P.; Hesse, D.I.R. Virtual synchronous machine. In Proceedings of the 2007 9th International Conference on Electrical Power Quality and Utilisation, Barcelona, Spain, 9–11 October 2007; pp. 1–6.
17. Driesen, J.; Visscher, K. Virtual synchronous generators. In Proceedings of the 2008 IEEE Power and Energy Society General Meeting-Conversion and Delivery of Electrical Energy in the 21st Century, Pune, India, 29–31 August 2008; pp. 1–3.
18. Tayyebi, A.; Gross, D.; Adolfo, A.; Dörfler, F. Grid-Forming Converter Control Techniques and Interactions with Synchronous Machines—A Comparative Study. Available online: https://www.researchgate.net/profile/Ali_Tayyebi/publication/330968040_Grid-Forming_Converter_Control_Techniques_and_Interactions_with_Synchronous_Machines_--_A_Comparative_Study/links/5c5d9755299bf1d14cb4b2a6/Grid-Forming-Converter-Control-Techniques-and-Interactions-with-Synchronous-Machines--A-Comparative-Study.pdf (accessed on 3 October 2020). [CrossRef]
19. Yan, X.; Mohamed, S.Y.A. Comparison of virtual synchronous generators dynamic responses. In Proceedings of the 2018 IEEE 12th International Conference on Compatibility, Power Electronics and Power Engineering (CPE-POWERENG 2018), Doha, Qatar, 10–12 April 2018; pp. 1–6.
20. Soni, N.; Doolla, S.; Chandorkar, M.C. Improvement of Transient Response in Microgrids Using Virtual Inertia. *IEEE Trans. Power Deliv.* **2013**, *28*, 1830–1838. [CrossRef]
21. RTDS Technologies Inc., The Simulator-Hardware. Available online: https://www.rtds.com/thesimulator/our-hardware (accessed on 3 October 2020).
22. RTDS Technologies Inc., RSCAD Modules. Available online: https://www.rtds.com/thesimulator/our-software/rscad-modules (accessed on 3 October 2020).
23. Fang, J.; Li, H.; Tang, Y.; Blaabjerg, F. On the Inertia of Future More-Electronics Power Systems. *IEEE J. Emerg. Sel. Top. Power Electron.* **2019**, *7*, 2130–2146. [CrossRef]
24. Mohapatra, T.K.; Sahu, B.K. Design and implementation of SSA based fractional order PID controller for automatic generation control of a multi-area, multi-source interconnected power system. In Proceedings of the 2018 Technologies for Smart-City Energy Security and Power (ICSESP), Bhubaneswar, India, 28–30 March 2018; pp. 1–6. [CrossRef]
25. Gonzalez-Longatt, F.M.; Bonfiglio, A.; Procopio, R.; Verduci, B. Evaluation of inertial response controllers for full-rated power converter wind turbine (Type 4). In Proceedings of the 2016 IEEE Power and Energy Society General Meeting (PESGM), Boston, MA, USA, 17–21 July 2016; pp. 1–5.
26. International Review of Frequency Control Adaptation, Australia Energy Market Operator. Melbourne, VIC, Australia. 2017. Available online: http://www.aemo.com.au (accessed on 3 October 2020).
27. Modig, N.; Eriksson, R.; Haarla, L.; Ruokolainen, P.; Kuivaniemi, M.; Hornnes, K.S.; Vada, P.A.; Meybodi, S.A.; Karlsson, D. *Technical Requirements for Fast Frequency Reserve Provision in the Nordic Synchronous Area*; Techical Report for Fingrid; Fingrid: Helsinki, Finland, July 2019; Available online: electricenergyonline.com/article/energy/category/t-d/56/778092/technical-requirements-for-fast-frequency-reserve-have-been-published.html (accessed on 3 October 2020).

28. Nikolopoulou, A. Wind Turbine Contribution to Ancillary Services under Increased Renewable Penetration levels. Master's Thesis, Delft University of Technology, Delft, The Netherlands, September 2017. Available online: https://repository.tudelft.nl/islandora/object/uuid%3A321a3ff0-5c7a-4c33-a891-4f0233c32ac9 (accessed on 3 October 2020).
29. Oak Ridge National Laboratory. Frequency Control Concerns In The North American Electric Power System. Available online: https://info.ornl.gov/sites/publications/Files/Pub57419.pdf (accessed on 3 October 2020).